Structure and Magnetism of Novel Tetranuclear μ_4-Oxo-bridged Copper(II) Complexes

Jörg Reim,[a] Klaus Griesar,[b] Wolfgang Haase[b] and Bernt Krebs*[,a]

[a] *Anorganisch-Chemisches Institut der Universität Münster, Wilhelm-Klemm-Strasse 8, D-48149 Münster, Germany*

[b] *Institut für Physikalische Chemie der Technischen Hochschule Darmstadt, Petersenstrasse 20, D-64287 Darmstadt, Germany*

Reaction of $CuCl_2 \cdot 2H_2O$ or $CuBr_2$ with the tridentate ligand 4-methyl-2,6-bis(pyrrolidin-1-ylmethyl)phenol (Hmbpp) in methanol yielded two copper(II) complexes $[Cu_4OCl_4(mbpp)_2] \cdot 2MeOH$ **1** and $[Cu_4OBr_4(mbpp)_2]$ **2**. They were characterised by single-crystal X-ray diffraction analyses. Both structures were solved using direct methods and refined on F^2 by full-matrix least squares. They consist of a tetrahedron of copper atoms centred by a μ_4-bridging oxygen atom. Magnetic susceptibility measurements in the temperature range 7.0–487.3 K indicated significant antiferromagnetic coupling between the copper(II) centres of both complexes. The experimental data were fitted to a modified Heisenberg model by analysing the tetranuclear complexes as two dinuclear Cu_2O_2 subunits. The best least-squares fit parameters were $g = 2.12(2)$, $J_{12} = -275(1)$ cm^{-1}, $J_{13} = -27.8(5)$ cm^{-1} and $x_p = 1.0(1)\%$ paramagnetic impurity for **1** and $g = 2.10(2)$, $J_{12} = -261(1)$ cm^{-1}, $J_{13} = -21.6(5)$ cm^{-1} and $x_p = 1.2(1)\%$ for **2**. By comparison to similar μ_4-oxo-bridged copper(II) complexes, a linear relationship between the magnetic intradimer coupling constant and the mean Cu–O–Cu angle is obtained.

Polynuclear complexes of paramagnetic transition-metal ions and their magnetic properties have attracted the attention of inorganic chemists for many years.[1,2] In biological systems, polynuclear metal centres at the active sites of a number of metalloproteins are abundant. Prominent examples are the iron-storage protein ferritin,[3a] the tetranuclear manganese cluster in photosystem II[3b] or the multicopper active sites in several oxidases.[3c] Particular interest has been directed towards the exchange phenomena in di- and poly-nuclear complexes of copper(II), studies of which have led to essential insights into magnetostructural correlations. Several structural parameters are important for the type and magnitude of the exchange interaction, such as the identity of the bridging chemical entities, the distance between the paramagnetic centres, the angles at the bridging atoms, the metal–bridge ligand bond lengths or the stereochemistry around the metal ion.[4]

Special attention has been drawn to tetranuclear μ_4-oxo-bridged copper(II) complexes of general formula $[Cu_4OX_{10-n}L_n]^{n-4}$ (X = Br or Cl; L = Lewis-base ligand). After Bertrand and Kelley[5] structurally characterised the first complex of this type, a number of further compounds of formulas $[Cu_4OX_6L_4]$ and $[Cu_4OX_{10}]^{4-}$ have been reported.[6] The complex ion $[Cu_4OCl_{10}]^{4-}$ is highly symmetric with an almost perfect tetrahedron of copper atoms around the central μ_4-oxygen atom.[7] The co-ordination polyhedra of the copper centres are nearly ideally trigonal bipyramidal. Replacement of the terminal chloride ligands by oxygen or nitrogen donors leads to significant deviations from the D_{3h} symmetry. Furthermore, this results in a characteristic distortion of the Cu_4 tetrahedron in complexes of the type $[Cu_4OCl_6L_4]$.[6g] By employing the tridentate amino alcohol ligand 4-methyl-2,6-bis(morpholinomethyl)phenol (Hmbmp) it was possible to prepare two tetramers of the type $[Cu_4OX_4L_6]$: $[Cu_4OBr_4(mbmp)_2] \cdot 2MeOH$ and $[Cu_4O(O_2CPh)_4(mbmp)_2] \cdot H_2O$.[8] In the latter compound, for the first time, all halide ions were replaced. Owing to the steric force of the chelating ligand, strong perturbations in the Cu_4O framework and in the copper co-ordination polyhedra were observed.

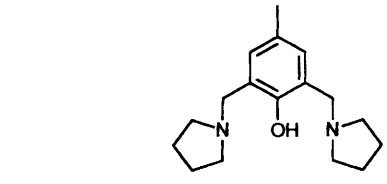

Hmbpp

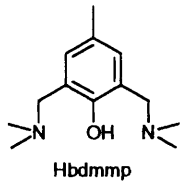

Hbdmmp

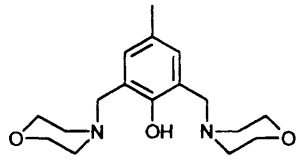

Hmbmp

To explain the magnetic behaviour of these complexes, which are strongly antiferromagnetically coupled, they were consequently simplified as a central Cu_4O_3 core, which could be described as two μ_4-O-connected Cu_2O_2 rings. Two coupling constants J_{12} and J_{13} were used describing the intra- and inter-dimer exchange phenomena, respectively. It was suggested that, for complexes which can be magnetically divided into Cu_2O_2 subunits, exchange coupling interactions will also follow known magnetostructural relationships. Recently, Chen *et al.*[9] reported a complex of formula $[Cu_4O(O_2CCF_3)_4(bdmmp)_2]$ {bdmmp = 2,6-bis[(dimethylamino)methyl]-4-methylpheno-

† *Supplementary data available:* see Instructions for Authors, *J. Chem. Soc., Dalton Trans.*, 1995, Issue 1, pp. xxv–xxx.

Non-SI unit employed: $\mu_B \approx 9.27 \times 10^{-24}$ J T^{-1}.

late}. Its magnetic behaviour was explained with a similar model, however two interdimer coupling constants were introduced because of a different bridging mode of the carboxylate ligands.

By variation of the structural parameters within the Cu_4O_3 core of this class of compounds, it should be possible to study correlations between structural details and the magnetic interaction. For this purpose, knowledge of a series of well characterised complexes, both structurally and magnetically, is necessary. Therefore, we have synthesised two novel tetranuclear μ_4-oxo-bridged copper(II) complexes with the tridentate dinucleating ligand 4-methyl-2,6-bis(pyrrolidin-1-ylmethyl)-phenol (Hmbpp). Here we report details on the syntheses, structural characterisation, magnetic and spectroscopic properties of $[Cu_4OCl_4(mbpp)_2]\cdot 2MeOH$ **1** and $[Cu_4OBr_4(mbpp)_2]$ **2**. The relation between structural features and the magnetic behaviour is discussed.

Results and Discussion

Syntheses of the Complexes.—The complexes $[Cu_4OCl_4(mbpp)_2]\cdot 2MeOH$ **1** and $[Cu_4OBr_4(mbpp)_2]$ **2** are obtained by reaction of $CuCl_2\cdot 2H_2O$ and $CuBr_2$, respectively, with the tridentate dinucleating ligand 4-methyl-2,6-bis(pyrrolidin-1-ylmethyl)phenol (Hmbpp) in aqueous methanol. Water serves as a source for the μ_4-oxo ligand. The compound Hmbpp is easily accessible by a Mannich reaction between *p*-cresol, formaldehyde and pyrrolidine.[10] The structures of both complexes were determined by single-crystal X-ray diffraction studies. The formulas of **1** and **2** are in accord with their elemental analyses.

Molecular Structure of $[Cu_4OCl_4(mbpp)_2]\cdot 2MeOH$ **1**.—A perspective view of the molecule in complex **1** is presented in Fig. 1 together with the atomic labelling system; Fig. 2 shows the central co-ordination unit for greater clarity. Selected interatomic distances and bond angles are collected in Table 1. The complex consists of a tetrahedron of four copper(II) atoms co-ordinating a central μ_4-oxygen atom. Four edges of the Cu_4 tetrahedron are bridged by chlorine atoms whereas the two remaining ones are bridged by the phenoxo group of the deprotonated ligand $mbpp^-$. The pyrrolidine groups of $mbpp^-$ are bound as terminal ligands to each of the copper atoms. While the lengths of the chloro-bridged edges show values between 3.182(1) [Cu(1) · · · Cu(4)] and 3.240(1) Å [Cu(2) · · · Cu(4)], the phenoxo-bridged edges are significantly shorter [Cu(1) · · · Cu(2) 2.996(1) and Cu(3) · · · Cu(4) 2.980(1) Å]. This strong perturbation of the tetrahedral co-ordination of the central oxygen O(2) is also reflected in the bond angles: two small angles of 102.19(7) [Cu(1)–O(2)–Cu(2)] and 101.68(7)° [Cu(3)–O(2)–Cu(4)], and four larger angles in the range from 111.40(8) [Cu(1)–O(2)–Cu(4)] to 115.22(8)° [Cu(2)–O(2)–Cu(4)] are observed. This strong distortion is attributed to the steric force of the chelating ligand.

Similar distortions with related ligands have been reported for the structures of $[Cu_4OBr_4(mbmp)_2]\cdot 2MeOH$ **3**,[8] $[Cu_4O(O_2CPh)_4(mbmp)_2]\cdot H_2O$ **4**[8] and $[Cu_4O(O_2CCF_3)_4(bdmmp)_2]$ **5**.[9] Each copper atom is in a NO_2Cl_2 donor set. A description of the geometry of the five-co-ordinated centres can be obtained determining the structural index τ defined by Addison *et al.*[11] It shows the relative amount of trigonality (square pyramid, $\tau = 0$; trigonal bipyramid, $\tau = 1$) where $\tau = (\beta - \alpha)/60°$, α and β being the two largest angles around the central atom. Application of this method yields values of τ between 0.23 [Cu(1)] and 0.28 [Cu(2)]. The co-ordination geometry of the copper centres is therefore best described as distorted square pyramidal with a chlorine atom at the apex. Two sets of copper–chlorine distances can be differentiated. The axial chlorine atoms have distances between 2.902(1) [Cu(2)–Cl(3)] and 3.015(1) Å [Cu(4)–Cl(2)] which are considerably longer than those of the equatorial bound chlorine

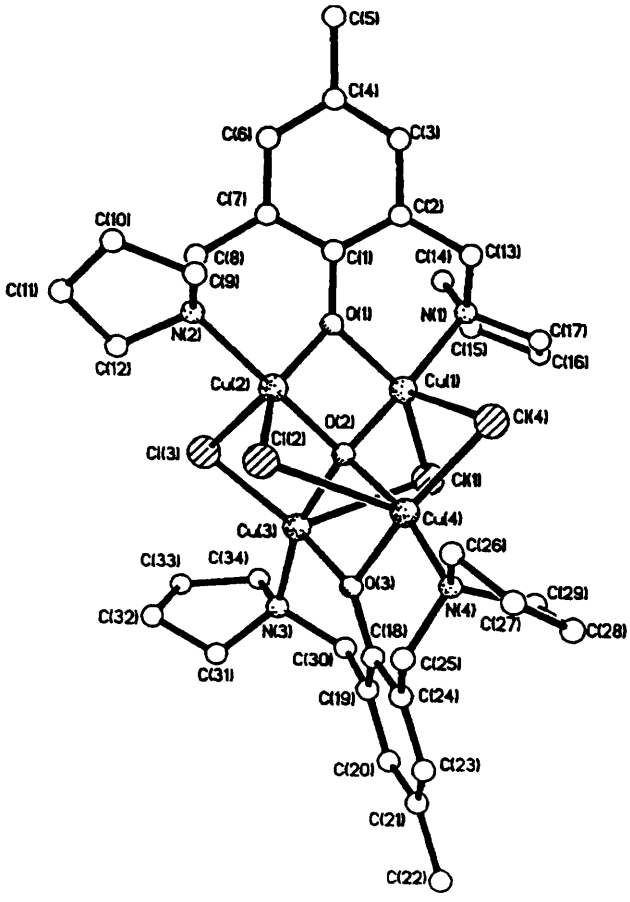

Fig. 1 Molecular structure and atomic numbering scheme for $[Cu_4OCl_4(mbpp)_2]$ in **1**. Hydrogen atoms are omitted for clarity

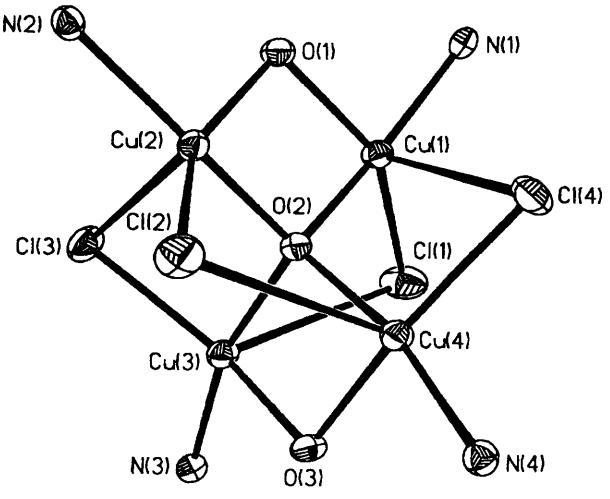

Fig. 2 The core of complex **1** showing 50% probability thermal ellipsoids

atoms {2.248(1) [Cu(4)–Cl(4)]–2.263(1) Å [Cu(3)–Cl(3)]}. The chlorine atoms are bridging in such a way that an axial chlorine of the co-ordination sphere of one copper belongs to the basal plane of another copper. Numerous dichloro-bridged dicopper(II) compounds with this structural unit and with similar values for the copper–chlorine distances are known.[12] However, in all μ_4-oxo-copper(II) complexes studied so far, no such asymmetric bridging of the chlorine atoms with distances up to 3.015(1) Å has been found. Owing to the symmetry of the $mbpp^-$ ligand and the equally surrounded metal centres, a symmetric environment of the μ-phenolato oxygen atoms O(1)

Table 1 Selected interatomic distances (Å) and angles (°) for complex **1**

Cu(1)···Cu(2)	2.996(1)	Cu(3)···Cu(4)	2.980(1)	Cu(2)–Cl(2)	2.252(1)	Cu(2)–Cl(3)	2.902(1)
Cu(1)···Cu(3)	3.229(1)	Cu(1)···Cu(4)	3.182(1)	Cu(3)–O(2)	1.924(2)	Cu(3)–O(3)	1.942(2)
Cu(2)···Cu(3)	3.205(1)	Cu(2)···Cu(4)	3.240(1)	Cu(3)–N(3)	2.024(2)	Cu(3)–Cl(3)	2.263(1)
Cu(1)–O(2)	1.932(2)	Cu(1)–O(1)	1.938(2)	Cu(3)–Cl(1)	2.959(1)	Cu(4)–O(2)	1.919(2)
Cu(1)–N(1)	2.017(2)	Cu(1)–Cl(1)	2.254(1)	Cu(4)–O(3)	1.956(2)	Cu(4)–N(4)	2.010(2)
Cu(1)–Cl(4)	2.947(1)	Cu(2)–O(2)	1.917(2)	Cu(4)–Cl(4)	2.248(1)	Cu(4)–Cl(2)	3.015(1)
Cu(2)–O(1)	1.960(2)	Cu(2)–N(2)	2.015(2)				
O(2)–Cu(1)–O(1)	78.73(7)	O(2)–Cu(1)–N(1)	163.87(7)	O(2)–Cu(3)–Cl(1)	71.09(5)	O(3)–Cu(3)–Cl(1)	93.34(6)
O(1)–Cu(1)–N(1)	92.03(7)	O(2)–Cu(1)–Cl(1)	89.69(5)	N(3)–Cu(3)–Cl(1)	96.59(6)	Cl(3)–Cu(3)–Cl(1)	110.98(3)
O(1)–Cu(1)–Cl(1)	150.29(5)	N(1)–Cu(1)–Cl(1)	104.44(6)	O(2)–Cu(4)–O(3)	79.08(7)	O(2)–Cu(4)–N(4)	167.80(7)
O(2)–Cu(1)–Cl(4)	72.97(5)	O(1)–Cu(1)–Cl(4)	98.07(6)	O(3)–Cu(4)–N(4)	93.28(7)	O(2)–Cu(4)–Cl(4)	92.28(5)
N(1)–Cu(1)–Cl(4)	95.58(6)	Cl(1)–Cu(1)–Cl(4)	104.59(3)	O(3)–Cu(4)–Cl(4)	153.88(5)	N(4)–Cu(4)–Cl(4)	98.57(6)
O(2)–Cu(2)–O(1)	78.55(7)	O(2)–Cu(2)–N(2)	166.62(7)	O(2)–Cu(4)–Cl(2)	71.26(5)	O(3)–Cu(4)–Cl(2)	93.93(5)
O(1)–Cu(2)–N(2)	93.56(7)	O(2)–Cu(2)–Cl(2)	92.06(5)	N(4)–Cu(4)–Cl(2)	100.09(6)	Cl(4)–Cu(4)–Cl(2)	106.68(3)
O(1)–Cu(2)–Cl(2)	149.86(5)	N(2)–Cu(2)–Cl(2)	99.97(6)	Cu(1)–Cl(1)–Cu(3)	75.20(3)	Cu(2)–Cl(2)–Cu(4)	74.32(3)
O(2)–Cu(2)–Cl(3)	72.78(5)	O(1)–Cu(2)–Cl(3)	92.75(5)	Cu(3)–Cl(3)–Cu(2)	75.59(3)	Cu(4)–Cl(4)–Cu(1)	74.17(3)
N(2)–Cu(2)–Cl(3)	97.09(6)	Cl(2)–Cu(2)–Cl(3)	111.92(3)	Cu(1)–O(1)–Cu(2)	100.42(7)	Cu(2)–O(2)–Cu(4)	115.22(8)
O(2)–Cu(3)–O(3)	79.31(7)	O(2)–Cu(3)–N(3)	164.44(7)	Cu(2)–O(2)–Cu(3)	113.12(8)	Cu(4)–O(2)–Cu(3)	101.68(7)
O(3)–Cu(3)–N(3)	92.32(7)	O(2)–Cu(3)–Cl(3)	89.88(5)	Cu(2)–O(2)–Cu(1)	102.19(7)	Cu(4)–O(2)–Cu(1)	111.40(8)
O(3)–Cu(3)–Cl(3)	148.65(5)	N(3)–Cu(3)–Cl(3)	103.71(6)	Cu(3)–O(2)–Cu(1)	113.71(8)	Cu(3)–O(3)–Cu(4)	99.76(7)

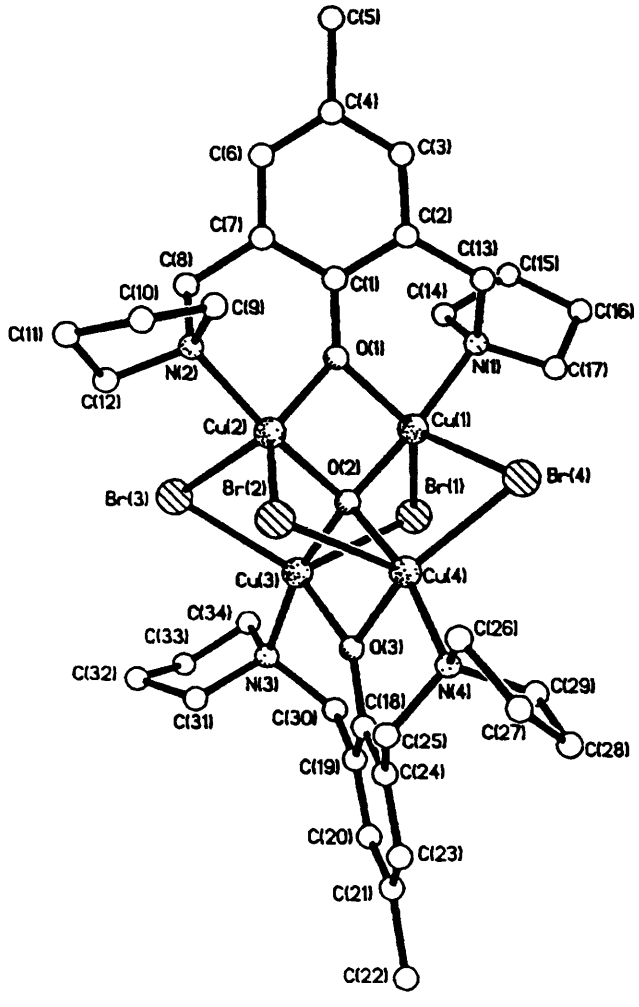

Fig. 3 Molecular structure and atomic numbering scheme for complex **2**. Hydrogen atoms are omitted for clarity

and O(3) is expected. In contrast to this, the Cu(1)–O(1)–C(1) angle is 130.6(2) and Cu(2)–O(1)–C(1) is 125.8(1)°. Similar values are observed around O(3): 130.5(1)° for Cu(3)–O(3)–C(18) and 125.1(1)° for Cu(4)–O(3)–C(18).

Molecular Structure of $[Cu_4OBr_4(mbpp)_2]$ **2**.—A perspective view of complex **2** is depicted in Fig. 3 along with the atomic numbering scheme. Selected interatomic distances and angles are given in Table 2. The structure of **2** is closely related to that of **1**. The chlorine atoms are replaced by bromine atoms. As in **1** the central Cu_4 tetrahedron is strongly distorted. While the bromine-bridged edges have lengths between 3.165(1) [Cu(1)···Cu(3)] and 3.247(1) Å [Cu(1)···Cu(4)], the phenoxo-bridged edges show values of 2.987(1) [Cu(1)···Cu(2)] and 3.006(1) Å [Cu(3)···Cu(4)]. Two angles around the μ_4-oxygen O(2) are significantly smaller than the ideal tetrahedral angle [102.4(2)° for Cu(1)–O(2)–Cu(2) and 103.2(2)° for Cu(3)–O(2)–Cu(4)]; the other four are larger [in the range 111.4(2)–115.7(2)°]. So the amount of distortion of the tetrahedron is similiar to that in **1**. The copper atoms are in a NO_2Br_2 environment. In analogy to **1**, two different sets of copper–halogen bond lengths are observed. However, here the difference is much less marked: the short distances are between 2.427(1) [Cu(1)–Br(1)] and 2.447(1) Å [Cu(3)–Br(3)] and the long distances lie in the range 2.753(1) [Cu(4)–Br(2)]–2.887(1) Å [Cu(1)–Br(4)]. The co-ordination geometry of the copper centres is intermediate between square pyramidal and trigonal bipyramidal, as indicated by the τ values of 0.48 [Cu(4)]–0.58 [Cu(3)]. In contrast to the situation in **1**, the phenolato oxygen atoms O(1) and O(3) are symmetrically surrounded.

Magnetic Properties.—Variable-temperature magnetic susceptibility data were obtained for solid samples of complexes **1** and **2** in the temperature range 7.0–487.3 K. The data are displayed as molar susceptibility and μ_{eff} *versus* temperature for **1** and **2** in Figs. 4 and 5, respectively. The curves are typical for antiferromagnetically coupled systems; the rise of the susceptibility at low temperature is caused by paramagnetic impurities. The antiferromagnetic exchange interaction is also expressed by the low room-temperature magnetic moments per copper of $\mu_{eff} = 0.97\ \mu_B$ for **1** and 1.01 μ_B for **2**.

Since the average Cu–X–Cu (X = Br or Cl) distances are relatively large in complexes **1** and **2**, a significant magnetic exchange contribution *via* this pathway can be excluded. This is confirmed by magnetostructural correlations.[13] So the only possible pathways allowing a magnetic interaction are $Cu–O_{phenolate}–Cu$ and $Cu–O_{oxo}–Cu$. The structures of **1** and **2** can therefore be reduced to a central Cu_4O_3 core which can be described as two μ_4-O-connected Cu_2O_2 rings (see Fig. 6). The coupling within the dinuclear Cu_2O_2 subunit is expected to be larger than the interdimer exchange interaction *via* the μ_4-

Table 2 Selected interatomic distances (Å) and angles (°) for complex **2**

Cu(1)···Cu(2)	2.987(1)	Cu(3)···Cu(4)	3.006(1)	Cu(2)–Br(2)	2.429(1)	Cu(2)–Br(3)	2.806(1)
Cu(1)···Cu(3)	3.165(1)	Cu(1)···Cu(4)	3.247(1)	Cu(3)–O(2)	1.916(4)	Cu(3)–O(3)	1.967(4)
Cu(2)···Cu(3)	3.195(1)	Cu(2)···Cu(4)	3.174(1)	Cu(3)–N(3)	2.013(5)	Cu(3)–Br(3)	2.447(1)
Cu(1)–O(2)	1.916(4)	Cu(1)–O(1)	1.954(4)	Cu(3)–Br(1)	2.760(1)	Cu(4)–O(2)	1.920(4)
Cu(1)–N(1)	2.008(5)	Cu(1)–Br(1)	2.427(1)	Cu(4)–O(3)	1.974(4)	Cu(4)–N(4)	2.027(5)
Cu(1)–Br(4)	2.887(1)	Cu(2)–O(2)	1.917(4)	Cu(4)–Br(4)	2.446(1)	Cu(4)–Br(2)	2.753(1)
Cu(2)–O(1)	1.974(4)	Cu(2)–N(2)	2.002(5)				
O(2)–Cu(1)–O(1)	79.5(2)	O(2)–Cu(1)–N(1)	169.2(2)	O(2)–Cu(3)–Br(1)	80.1(1)	O(3)–Cu(3)–Br(1)	105.4(2)
O(1)–Cu(1)–N(1)	91.7(2)	O(2)–Cu(1)–Br(1)	89.4(1)	N(3)–Cu(3)–Br(1)	95.7(2)	Br(3)–Cu(3)–Br(1)	116.8(1)
O(1)–Cu(1)–Br(1)	137.3(1)	N(1)–Cu(1)–Br(1)	101.3(1)	O(2)–Cu(4)–O(3)	78.6(2)	O(2)–Cu(4)–N(4)	168.2(2)
O(2)–Cu(1)–Br(4)	77.1(1)	O(1)–Cu(1)–Br(4)	104.3(1)	O(3)–Cu(4)–N(4)	91.8(2)	O(2)–Cu(4)–Br(4)	89.2(1)
N(1)–Cu(1)–Br(4)	99.4(1)	Br(1)–Cu(1)–Br(4)	113.3(1)	O(3)–Cu(4)–Br(4)	139.4(2)	N(4)–Cu(4)–Br(4)	102.6(2)
O(2)–Cu(2)–O(1)	79.0(2)	O(2)–Cu(2)–N(2)	170.7(2)	O(2)–Cu(4)–Br(2)	80.6(1)	O(3)–Cu(4)–Br(2)	104.4(2)
O(1)–Cu(2)–N(2)	92.4(2)	O(2)–Cu(2)–Br(2)	89.7(1)	N(4)–Cu(4)–Br(2)	95.3(1)	Br(4)–Cu(4)–Br(2)	111.7(1)
O(1)–Cu(2)–Br(2)	140.7(1)	N(2)–Cu(2)–Br(2)	99.3(2)	Cu(1)–Br(1)–Cu(3)	74.9(1)	Cu(2)–Br(2)–Cu(4)	75.3(1)
O(2)–Cu(2)–Br(3)	80.0(1)	O(1)–Cu(2)–Br(3)	102.7(1)	Cu(3)–Br(3)–Cu(2)	74.6(1)	Cu(4)–Br(4)–Cu(1)	74.5(1)
N(2)–Cu(2)–Br(3)	98.5(1)	Br(2)–Cu(2)–Br(3)	112.3(1)	Cu(1)–O(1)–Cu(2)	99.0(2)	Cu(3)–O(2)–Cu(1)	111.4(2)
O(2)–Cu(3)–O(3)	78.9(2)	O(2)–Cu(3)–N(3)	168.4(2)	Cu(3)–O(2)–Cu(2)	112.9(2)	Cu(1)–O(2)–Cu(2)	102.4(2)
O(3)–Cu(3)–N(3)	92.0(2)	O(2)–Cu(3)–Br(3)	90.2(1)	Cu(3)–O(2)–Cu(4)	103.2(2)	Cu(1)–O(2)–Cu(4)	115.7(2)
O(3)–Cu(3)–Br(3)	133.7(2)	N(3)–Cu(3)–Br(3)	101.4(2)	Cu(2)–O(2)–Cu(4)	111.6(2)	Cu(3)–O(3)–Cu(4)	99.4(2)

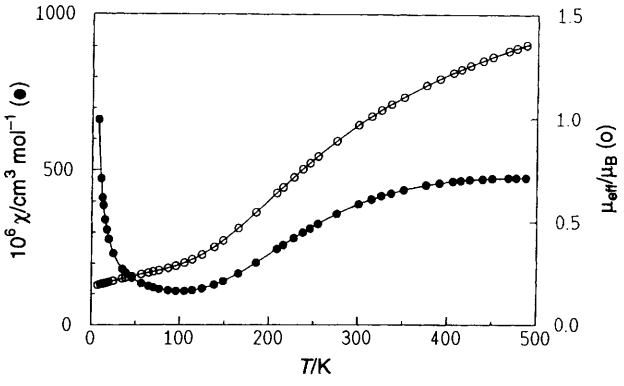

Fig. 4 Variation of the experimental data for χ (●) and μ_{eff} (○) with temperature and calculated values (—) for $[Cu_4OCl_4(mbpp)_2]\cdot 2MeOH$ **1**

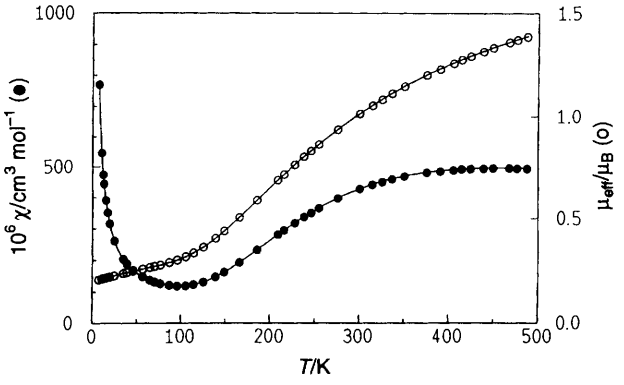

Fig. 5 Variation of the experimental data for χ (●) and μ_{eff} (○) with temperature and calculated values (—) for $[Cu_4OBr_4(mbpp)_2]$ **2**

oxygen atom. Hence the exchange interaction in the tetrameric unit represented by Fig. 6 may be explained by the Heisenberg Hamiltonian (1) where $\hat{S}_1$, $\hat{S}_2$, $\hat{S}_3$ and $\hat{S}_4$ are the spin operators

$$\hat{H} = -2(J_{12}\hat{S}_1\hat{S}_2 + J_{13}\hat{S}_1\hat{S}_3 + J_{14}\hat{S}_1\hat{S}_4 + J_{23}\hat{S}_2\hat{S}_3 + J_{24}\hat{S}_2\hat{S}_4 + J_{34}\hat{S}_3\hat{S}_4) \quad (1)$$

for the four copper centres, J_{12} and J_{34} are the intradimer interactions and J_{13}, J_{23}, J_{14} and J_{24} are the various interdimer interactions. Considering chemically similar environments to be

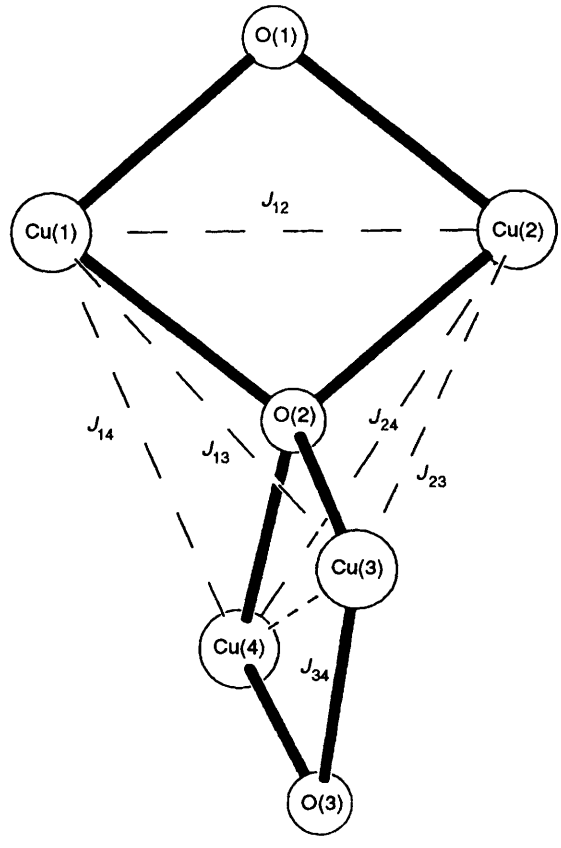

Fig. 6 The magnetic exchange interaction within the central Cu_4O_3 core

magnetically equivalent, equation (1) degenerates directly to equation (2), which means $J_{12} = J_{34}$ and $J_{13} = J_{14} = J_{23} = J_{24}$. The susceptibility can be expressed theoretically by equation (3), with $x = J_{12}/kT$ and $y = J_{13}/kT$. Here N_α represents the temperature-independent paramagnetism which was set to 60×10^{-6} cm^3 mol^{-1} for each copper atom. A correction for a small amount (x_p) of paramagnetic impurity ($S = \frac{1}{2}$)

$$\hat{H} = -2[J_{12}(\hat{S}_1\hat{S}_2 + \hat{S}_3\hat{S}_4) + J_{13}(\hat{S}_1\hat{S}_3 + \hat{S}_1\hat{S}_4 + \hat{S}_2\hat{S}_3 + \hat{S}_2\hat{S}_4)] \quad (2)$$

Table 3 Crystallographic data and experimental details

	1	2
Formula	$C_{36}H_{58}Cl_4Cu_4N_4O_5$	$C_{34}H_{50}Br_4Cu_4N_4O_3$
M	1022.82	1136.58
Crystal system	Triclinic	Monoclinic
Space group	$P\bar{1}$	$P2_1/c$
a/Å	10.152(3)	13.225(3)
b/Å	10.257(2)	13.347(3)
c/Å	20.721(5)	22.326(4)
α/°	88.03(2)	
β/°	87.45(2)	91.14(3)
γ/°	76.27(2)	
U/Å^3	2093	3940
2θ range/°	4.5–54.1	4.3–54.1
Lattice segment	$+h, \pm k, \pm l$	$+h, +k, \pm l$
Z	2	4
T/K	150	293
D_c/g cm^{-3}	1.623	1.916
$F(000)$	1052	2248
Crystal size/mm	0.42 × 0.37 × 0.17	0.27 × 0.22 × 0.12
Crystal shape and colour	Dark green block	Dark green rhombus
μ/mm^{-1}	2.31	6.23
Absorption correction[a]	ψ Scan, empirical	ψ Scan, empirical
Maximum, minimum transmission factors	0.675, 0.379	0.474, 0.186
Unique data	9104	8014
Observed data [$I > 2\sigma(I)$]	7279	4499
Number of parameters	498	444
$R1$ [$I > 2\sigma(I)$], $wR2$ (all data)[b]	0.0282, 0.0701	0.0451, 0.1009
Weighting scheme, w^{-1}[c]	$\sigma^2(F_o^2) + (0.0395P)^2$	$\sigma^2(F_o^2) + (0.0432P)^2$

[a] XEMP.[22] [b] $R1 = \Sigma||F_o| - |F_c||/\Sigma|F_o|$, $wR2 = [\Sigma w(F_o^2 - F_c^2)^2/\Sigma w(F_o^2)^2]^{\frac{1}{2}}$. [c] $P = (F_o^2 + 2F_c^2)/3$.

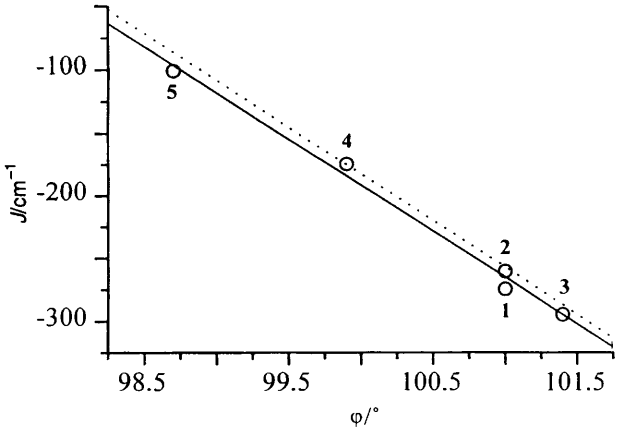

Fig. 7 Plot of intradimer coupling constant J *versus* mean Cu–O–Cu bridge angle φ together with the correlation curves for the discussed μ_4-oxo copper(II) complexes (—) and for di-μ-hydroxo-copper(II) complexes (. . .)

$$\chi_{Cu_4} = (1 - x_p)\frac{Ng^2\mu^2}{kT}\{[10\exp(2x) + 2\exp(-2x) + 4\exp(-2y)]/[5\exp(2x) + 3\exp(-2x) + \exp(-4x) + 6\exp(-2y) + \exp(-4y)]\} + \exp\left(\frac{Ng^2\mu^2}{3kT}\right)S(S+1) + N_\alpha \quad (3)$$

was also taken into account. The best parameters which were obtained using a standard least-squares fitting program were $g = 2.12(2)$, $J_{12} = -275(1)$ cm^{-1}, $J_{13} = -27.8(5)$ cm^{-1} and $x_p = 1.0(1)\%$ for **1** and $g = 2.10(2)$, $J_{12} = -261(1)$ cm^{-1}, $J_{13} = -21.6(5)$ cm^{-1} and $x_p = 1.2(1)\%$ for **2**. The discrepancy values, defined as $R = \Sigma|\chi_{obs} - \chi_{calc}|/\Sigma\chi_{obs}$, were 0.43 for **1** and 0.60 for **2**. The susceptibility data consistent with this set were found to be relatively insensitive to J_{13} but very sensitive to J_{12}. Measurement of susceptibility data at higher temperatures up to 478 K was necessary to determine J_{13} accurately. Excited magnetic states contribute significantly to the magnetic susceptibilities[8] only at higher temperatures.

Intensive studies on dimeric copper(II) complexes have pointed out that magnetic exchange interactions can be correlated to structural parameters.[13] For symmetrically bridged dicopper(II) hydroxo complexes a linear relationship between the exchange integral and Cu–O–Cu bridge angle is well established.[14] For Cu–O–Cu angles less than 97.5° the copper centres should be ferromagnetically coupled. An opening of the angle is connected with a transition from ferromagnetic to antiferromagnetic coupling. A similar correlation exists for alkoxo-bridged copper(II) dimers[15] and also for unsymmetrically μ-phenoxo-bridged copper(II) complexes with exchangeable exogenic ligands.[16]

Since the tetrameric μ_4-oxo complexes can be treated as dimeric subunits, an explanation of the magnetic properties in terms of magnetostructural correlations is possible. Similarly, in the case of iron(III) centres bridged by a ligand oxygen atom (oxo, hydroxo, alkoxo) the quantitative magnetostructural relationships which have been found for dinuclear complexes have been successfully applied to polynuclear iron clusters.[17] In addition to **1** and **2**, structural and magnetic details for the three closely related compounds $[Cu_4OBr_4(mbmp)_2]\cdot 2MeOH$ **3**,[8] $[Cu_4O(O_2CPh)_4(mbmp)_2]\cdot H_2O$ **4**[8] and $[Cu_4O(O_2CCF_3)_4(bdmmp)_2]$ **5**[9] are available. The complexes of this series also have the same electronic structures, since the bridging atoms within the dimeric subunits are a μ_4-oxygen and a μ-oxygen stemming from a *p*-cresol group. As shown in Fig. 7, there is a good correlation between the intradimer coupling constant and the mean Cu–O–Cu bridge angle φ within the Cu_2O_2 subunits. For both complexes **1** and **2**, the angle φ is 101.0°. The J values for complexes **3**–**5** are −296, −175 and −101 cm^{-1}, respectively and the corresponding φ values are reported as 101.4, 99.9 and 98.7°. A standard linear regression analysis yields equation (4) with a correlation coefficient, R, of −0.996

$$J/\text{cm}^{-1} = -73.54\varphi + 7162 \quad (4)$$

Table 4 Final positional parameters for complex **1**

Atom	*x*	*y*	*z*	Atom	*x*	*y*	*z*
Cu(1)	−0.114 00(3)	0.510 46(3)	0.247 80(1)	C(11)	0.410 6(3)	0.340 2(3)	0.014 5(1)
Cu(2)	0.162 45(3)	0.421 58(3)	0.184 40(1)	C(12)	0.334 0(3)	0.427 4(3)	0.069 5(1)
Cu(3)	0.102 62(3)	0.690 04(3)	0.266 40(1)	C(13)	−0.247 2(2)	0.310 1(2)	0.211 5(1)
Cu(4)	0.135 44(3)	0.431 01(3)	0.340 63(1)	C(14)	−0.380 6(2)	0.537 7(2)	0.187 0(1)
Cl(1)	−0.180 40(7)	0.693 92(7)	0.308 81(3)	C(15)	−0.462 3(3)	0.653 6(3)	0.226 5(1)
Cl(2)	0.353 77(6)	0.337 07(7)	0.237 75(3)	C(16)	−0.477 1(3)	0.592 8(3)	0.294 1(1)
Cl(3)	0.123 17(7)	0.707 48(6)	0.157 46(3)	C(17)	−0.369 9(2)	0.458 7(2)	0.296 3(1)
Cl(4)	−0.004 62(7)	0.291 01(6)	0.340 33(3)	C(18)	0.198 0(2)	0.663 0(2)	0.402 4(1)
O(1)	−0.027 8(2)	0.425 3(2)	0.169 7(1)	C(19)	0.143 6(2)	0.799 6(2)	0.412 2(1)
O(2)	0.073 3(2)	0.512 6(2)	0.259 3(1)	C(20)	0.172 1(2)	0.853 5(2)	0.469 8(1)
O(3)	0.176 2(2)	0.607 1(2)	0.346 8(1)	C(21)	0.249 5(2)	0.775 7(2)	0.517 1(1)
O(4)	−0.180 4(2)	0.717 3(2)	0.112 6(1)	C(22)	0.277 4(3)	0.836 3(3)	0.579 1(1)
O(5)	−0.443 8(4)	0.938 8(3)	0.343 3(2)	C(23)	0.300 1(2)	0.639 6(2)	0.505 8(1)
O(5′)	−0.445 7(14)	1.066 6(13)	0.217 0(7)	C(24)	0.276 6(2)	0.581 9(2)	0.448 7(1)
N(1)	−0.286 7(2)	0.452 5(2)	0.233 5(1)	C(25)	0.339 1(2)	0.436 9(2)	0.434 2(1)
N(2)	0.225 7(2)	0.360 0(2)	0.094 6(1)	C(26)	0.312 4(2)	0.214 1(2)	0.409 4(1)
N(3)	0.101 9(2)	0.876 2(2)	0.295 9(1)	C(27)	0.346 3(3)	0.151 7(3)	0.476 2(1)
N(4)	0.237 0(2)	0.357 3(2)	0.420 1(1)	C(28)	0.232 0(4)	0.229 2(3)	0.520 2(1)
C(1)	−0.072 3(2)	0.349 9(2)	0.127 3(1)	C(29)	0.150 1(3)	0.344 5(2)	0.479 5(1)
C(2)	−0.181 9(2)	0.294 1(2)	0.144 2(1)	C(30)	0.049 6(2)	0.884 9(2)	0.364 7(1)
C(3)	−0.225 1(2)	0.217 2(2)	0.098 9(1)	C(31)	0.235 8(3)	0.914 3(2)	0.289 6(1)
C(4)	−0.160 0(2)	0.191 4(2)	0.038 5(1)	C(32)	0.244 5(3)	0.965 1(3)	0.220 0(1)
C(5)	−0.207 0(3)	0.106 0(3)	−0.010 0(1)	C(33)	0.098 4(3)	1.037 7(3)	0.206 3(1)
C(6)	−0.048 8(2)	0.247 5(2)	0.023 7(1)	C(34)	0.008 1(3)	0.980 4(2)	0.255 2(1)
C(7)	−0.004 8(2)	0.327 2(2)	0.066 9(1)	C(35)	−0.231 1(4)	0.849 8(3)	0.133 4(2)
C(8)	0.108 4(2)	0.395 5(2)	0.049 8(1)	C(36)	−0.417 0(6)	1.017 9(5)	0.289 1(3)
C(9)	0.295 0(2)	0.213 9(2)	0.090 6(1)	C(36′)	−0.396(7)	1.022(7)	0.291(4)
C(10)	0.382 2(3)	0.201 1(3)	0.027 5(1)				

Table 5 Final positional parameters for complex **2**

Atom	*x*	*y*	*z*	Atom	*x*	*y*	*z*
Cu(1)	0.842 60(6)	0.422 22(6)	0.189 96(3)	C(11)	0.460 9(6)	0.707 8(7)	0.058 6(3)
Cu(2)	0.667 45(5)	0.499 68(6)	0.117 18(3)	C(12)	0.556 0(5)	0.650 6(5)	0.050 2(3)
Cu(3)	0.818 60(6)	0.345 03(6)	0.056 37(3)	C(13)	0.844 9(5)	0.535 5(5)	0.298 0(3)
Cu(4)	0.669 01(5)	0.266 28(6)	0.144 37(3)	C(14)	1.006 6(5)	0.542 9(6)	0.245 2(3)
Br(1)	0.976 85(5)	0.335 48(7)	0.138 61(4)	C(15)	1.075 2(6)	0.547 0(7)	0.301 3(3)
Br(2)	0.518 68(5)	0.394 31(5)	0.104 97(3)	C(16)	1.051 9(6)	0.451 9(7)	0.335 3(4)
Br(3)	0.781 30(6)	0.509 32(6)	0.012 63(3)	C(17)	0.968 6(5)	0.400 0(5)	0.299 1(3)
Br(4)	0.707 35(7)	0.288 85(7)	0.251 16(3)	C(18)	0.740 7(5)	0.133 1(5)	0.044 9(3)
O(1)	0.764 7(3)	0.545 6(3)	0.179 5(2)	C(19)	0.825 0(5)	0.103 9(5)	0.012 8(3)
O(2)	0.749 5(3)	0.382 3(3)	0.127 6(2)	C(20)	0.826 0(5)	0.011 0(5)	−0.011 1(3)
O(3)	0.737 1(3)	0.224 4(3)	0.070 6(2)	C(21)	0.745 9(6)	−0.056 2(5)	−0.006 1(3)
N(1)	0.918 3(4)	0.479 1(4)	0.261 0(2)	C(22)	0.749 3(7)	−0.160 2(6)	−0.035 0(4)
N(2)	0.601 4(4)	0.634 4(4)	0.111 6(2)	C(23)	0.660 0(6)	−0.024 4(5)	0.025 3(3)
N(3)	0.892 7(4)	0.278 4(4)	−0.010 7(2)	C(24)	0.656 6(5)	0.070 5(5)	0.050 4(3)
N(4)	0.580 8(4)	0.142 1(4)	0.143 5(2)	C(25)	0.563 0(4)	0.110 1(5)	0.080 5(3)
C(1)	0.763 1(4)	0.629 3(4)	0.211 7(3)	C(26)	0.479 0(4)	0.161 0(5)	0.172 3(3)
C(2)	0.804 9(4)	0.630 8(5)	0.270 8(3)	C(27)	0.435 7(5)	0.057 0(5)	0.186 3(3)
C(3)	0.799 9(4)	0.719 4(5)	0.302 3(3)	C(28)	0.529 4(5)	−0.011 7(5)	0.192 0(3)
C(4)	0.755 6(5)	0.804 6(5)	0.279 3(3)	C(29)	0.620 5(5)	0.058 0(5)	0.181 6(3)
C(5)	0.748 3(6)	0.898 6(5)	0.317 6(4)	C(30)	0.914 9(5)	0.172 7(5)	0.008 2(3)
C(6)	0.718 0(5)	0.801 4(5)	0.221 3(3)	C(31)	0.833 6(5)	0.278 8(6)	−0.068 7(3)
C(7)	0.719 8(4)	0.716 1(5)	0.187 3(3)	C(32)	0.890 1(6)	0.344 7(6)	−0.110 4(3)
C(8)	0.680 6(5)	0.713 2(5)	0.123 9(3)	C(33)	0.998 8(6)	0.333 4(7)	−0.089 2(3)
C(9)	0.513 6(4)	0.646 8(5)	0.153 3(3)	C(34)	0.990 0(5)	0.333 0(5)	−0.023 5(3)
C(10)	0.424 1(6)	0.666 7(8)	0.115 1(3)				

and a standard deviation of 9 cm^{-1}. This equation is nearly identical to the empirical equation derived for symmetric planar di-μ-hydroxo-bridged copper(II) complexes.[14] For illustration, the straight line corresponding to this equation is also depicted in Fig. 7. Besides, for di-μ-hydroxo-copper(II) complexes a linear relationship between the Cu···Cu separation and the exchange integral has also been obtained.[14] However this is not the case for the class of compounds discussed here.

It is noteworthy that the correlation equation (4) is independent of the co-ordination geometry of the copper atoms. Whereas in complexes **4** and **5** the geometries of the metal centres are essentially square pyramidal, in **1** they are distorted square pyramidal, in **2** they are completely distorted between both cases and in **3** they are nearly trigonal bipyramidal. However, a change in the co-ordination geometry is accompanied by a change in the orientation of the d orbitals relative to the Cu_2O_2 plane.[8] As a consequence, the overlap of the p orbitals of the bridging oxygen atoms with the magnetic orbitals of the metal should be influenced.

The current study shows that the magnetic properties of μ_4-oxo-tetracopper(II) complexes can be correlated to one geometrical parameter. The magnetic coupling within the

dimeric unit follows known magnetostructural correlations derived for isolated di-μ-oxygen-bridged copper(II) complexes. A detailed theoretical investigation is necessary fully to understand the magnetic exchange interaction in these compounds.

Spectroscopic Studies.—The electronic absorption spectra of complexes **1** and **2** in dichloromethane solutions were recorded in the range 250–1000 nm. The intense absorptions below 300 nm are due to ligand $\pi \longrightarrow \pi^*$ transitions. They occur at λ = 296 (ε = 11 140 per ligand) for **1** and at 291 nm (13 580 dm^3 mol^{-1} cm^{-1} per ligand) for **2**. The assignment of bands in the charge-transfer region is more difficult. For both compounds, phenolate→Cu^{II} and halide→Cu^{II} charge-transfer bands are expected. The position of the phenolate charge-transfer band depends on the ligand environment, the presence of chelating ligands as well as on the electron density on the copper centre.[18,19] For μ-phenoxo-copper(II) dimers, phenolate→Cu^{II} bands have been reported to lie between 370 and 500 nm.[19,20] A similar wide range is known for halide→Cu^{II} charge-transfer transitions.[6c,20] In the spectrum of **1**, a shoulder at about 370 nm is interpreted as superposition of the phenolate→Cu^{II} and the chloride→Cu^{II} charge-transfer bands. The spectrum of **2** reveals two broad shoulders, at about 330 nm and at about 410 nm. As pointed out, it is not possible to distinguish between the phenolate→Cu^{II} and the bromide→Cu^{II} charge-transfer transitions. The ligand-field spectra of both complexes show broad bands, with maxima at λ = 727 (ε = 193 per Cu) for **1** and at 732 nm (ε = 313 dm^3 mol^{-1} cm^{-1} per Cu) for **2**. This is in accord with, first, the general rule that d–d transitions for square-pyramidal copper(II) ions are shifted to higher energies compared to trigonal-bipyramidal copper(II) ions,[21] and secondly, the higher ligand-field strength of chloride relative to bromide.

The IR spectra of the tetranuclear complexes are dominated by the bands of the organic ligand $mbpp^-$. Comparison with the spectrum of free Hmbpp shows a movement of ν(C–N) to higher wavenumbers (from 1037 to 1049 cm^{-1} for **1** and to 1050 cm^{-1} for **2**) due to the co-ordination of the pyrrolidine group to copper. In the low-energy region only the absorptions found at 583 (**1**) and 584 cm^{-1} (**2**) can definitely be assigned. They belong to the asymmetric vibration of the Cu_4O core which Bock *et al.*[6a] pointed out to be characteristic for μ_4-oxo-tetracopper(II) complexes.

Experimental

Materials and Methods.—All reagents were obtained from commercial sources and used as received. Electronic spectra were recorded on a Shimadzu UV-3100 spectrophotometer, infrared spectra in the range 4000–200 cm^{-1} on a Perkin-Elmer 683 spectrophotometer using KBr as a dilution matrix and FIR spectra (400–80 cm^{-1}) on a Bruker IF 113v instrument in a polyethylene matrix. Elemental analyses were performed at the Institute of Organic Chemistry, University of Münster. Magnetic susceptibilities of powdered samples were recorded on a Faraday-type magnetometer using a sensitive Cahn RG electrobalance in the temperature range 7.0–487.3 K. The magnetic field applied was ≈1.2 T. Details of the apparatus have been described elsewhere.[15] Experimental susceptibility data were corrected for the underlying diamagnetism. Corrections for diamagnetism were estimated as -885×10^{-6} and -918×10^{-6} cm^3 mol^{-1} for complexes **1** and **2**, respectively.

Syntheses.—4-Methyl-2,6-bis(pyrrolidin-1-ylmethyl)phenol (Hmbpp) was prepared as previously described.[10]

$[Cu_4OCl_4(mbpp)_2]\cdot 2MeOH$ **1**. To a solution of $CuCl_2\cdot 2H_2O$ (170 mg, 1 mmol) in methanol (25 cm^3) were added Hmbpp (137 mg, 0.5 mmol) and 0.5 mol dm^{-3} aqueous sodium hydroxide solution (1 cm^3, 0.5 mmol) while stirring. After 24 h the dark green crystals were filtered off and washed with methanol. Yield 110 mg, 43% (Found: C, 42.25; H, 5.70; N, 5.50. $C_{36}H_{58}Cl_4Cu_4N_4O_5$ requires C, 42.20; H, 5.55; N, 5.55%).

$[Cu_4OBr_4(mbpp)_2]$ **2**. A solution of $CuBr_2$ (112 mg, 0.5 mmol) in methanol (20 cm^3) was treated under stirring with Hmbpp (69 mg, 0.25 mmol) and 0.5 mol dm^{-3} aqueous sodium hydroxide solution (0.5 cm^3, 0.25 mmol). The mixture was allowed to stand for 24 h. The dark green crystals obtained, were filtered off and washed with methanol. Yield 78 mg, 27% (Found: C, 35.95; H, 4.45; N, 4.95. $C_{34}H_{50}Br_4Cu_4N_4O_3$ requires C, 35.85; H, 4.40; N, 4.95%).

X-Ray Methods and Structure Determinations.—Intensity data were collected on a Syntex $P2_1$ (**1**) and on a Siemens P3 (**2**) diffractometer (Mo-Kα radiation, λ = 0.710 73 Å, graphite monochromator) by using the ω-scan technique and a variable scan rate (2–29° min^{-1}). The intensities of two reflections were monitored and no significant crystal deterioration was observed. Further data collection parameters are summarised in Table 3. The structures were solved by using direct methods.[22] A series of full-matrix least-squares refinement cycles on F^2 (program SHELXL 93[23]) followed by Fourier syntheses gave all remaining atoms. The hydrogen atoms in both structures were placed at calculated positions and constrained to 'ride' on the atom to which they are attached. The isotropic thermal parameters for the methyl protons were refined with 1.5 times, and for all other hydrogen atoms with 1.2 times, the U_{eq} value of the corresponding atom. All other atoms of complexes **1** and **2** were refined anisotropically. With the exception of one disordered solvent molecule in **1** {K[C(36)] = K[O(5)] = 0.769(6), K[C(36′)] = K[O(5′)] = 0.231(6)} the occupancy factors for all other atoms in **1** and **2** are K = 1. The positions of the hydrogen atoms attached to C(36′) and O(5′) were not calculated; C(36′) was refined isotropically. Final atomic coordinates of compounds **1** and **2** are listed in Tables 4 and 5, respectively.

Additional material available from the Cambridge Crystallographic Data Centre comprises H-atom coordinates, thermal parameters and remaining bond lengths and angles.

Acknowledgements

This work was supported by the Deutsche Forschungsgemeinschaft and the Fonds der Chemischen Industrie.

References

1 O. Kahn, *Inorg. Chim. Acta*, 1982, **62**, 3; *Angew. Chem.*, 1985, **97**, 837; *Angew. Chem., Int. Ed. Engl.*, 1985, **24**, 834; *Struct. Bonding (Berlin)*, 1987, **68**, 89.
2 M. D. Glick and R. L. Lintvedt, *Prog. Inorg. Chem.*, 1976, **21**, 233.
3 (*a*) E. C. Theil, *Annu. Rev. Biochem.*, 1987, **56**, 289; (*b*) K. Wieghardt, *Angew. Chem.*, 1994, **106**, 765; *Angew. Chem., Int. Ed. Engl.*, 1994, **33**, 725; (*c*) E. I. Solomon, in *Copper Coordination Chemistry: Biochemical & Inorganic Perspectives*, Adenine Press, Guilderland, NY, 1983, pp. 1–22.
4 D. J. Hodgson, *Prog. Inorg. Chem.*, 1975, **19**, 173; R. J. Doedens, *Prog. Inorg. Chem.*, 1976, **21**, 209; M. Kato and Y. Muto, *Coord. Chem. Rev.*, 1988, **92**, 45.
5 J. A. Bertrand and J. A. Kelley, *J. Am. Chem. Soc.*, 1966, **88**, 4746; J. A. Bertrand, *Inorg. Chem.*, 1967, **6**, 495.
6 (*a*) H. Bock, H. tom Dieck, H. Pyttlik and M. Schnöller, *Z. Anorg. Allg. Chem.*, 1968, **357**, 54; (*b*) B. T. Kilbourn and J. D. Dunitz, *Inorg. Chim. Acta*, 1967, **1**, 209; (*c*) F. S. Keij, J. G. Haasnoot, A. J. Oosterling, J. Reedijk, C. J. O'Connor, J. H. Zang and A. L. Spek, *Inorg. Chim. Acta*, 1991, **181**, 185; (*d*) H. M. Haendler, *Acta Crystallogr., Sect. C*, 1990, **46**, 2054; (*e*) R. E. Norman, N. J. Rose and R. E. Stenkamp, *Acta Crystallogr., Sect. C*, 1989, **45**, 1707; (*f*) S. Brownstein, N. F. Han, E. Gabe and F. Leer, *Can. J. Chem.*, 1989, **67**, 551; (*g*) J. T. Guy, jun., J. C. Cooper, R. D. Gillardi, J. L. Flippen-Anderson and C. F. George, jun., *Inorg. Chem.*, 1988, **27**, 635; (*h*) M. R. Churchill and F. J. Rotella, *Inorg.*

Chem., 1979, **18**, 853; (*i*) R. C. Dickinson, F. T. Helm, W. A. Baker, jun., T. D. Black and W. H. Watson, jun., *Inorg. Chem.*, 1977, **16**, 1530 and refs. therein.
7 J. J. de Boer, D. Bright and J. N. Helle, *Acta Crystallogr., Sect. B*, 1972, **28**, 3436.
8 S. Teipel, K. Griesar, W. Haase and B. Krebs, *Inorg. Chem.*, 1994, **33**, 456.
9 L. Chen, S. R. Breeze, R. J. Rousseau, S. Wang and L. K. Thompson, *Inorg. Chem.*, 1995, **34**, 454.
10 J. Reim and B. Krebs, *Angew. Chem.*, 1994, **106**, 2040; *Angew. Chem., Int. Ed. Engl.*, 1994, **33**, 1969.
11 A. W. Addison, T. N. Rao, J. Reedijk, J. van Rijn and G. C. Verschoor, *J. Chem. Soc., Dalton Trans.*, 1984, 1349.
12 W. E. Marsh, W. E. Hatfield and D. J. Hodgson, *Inorg. Chem.*, 1982, **21**, 2679; W. E. Marsh, K. C. Patel, W. E. Hatfield and D. J. Hodgson, *Inorg. Chem.*, 1983, **22**, 511.
13 R. D. Willett, in *Magneto-Structural Correlations in Exchange Coupled Systems*, eds. R. D. Willett, D. Gatteschi and O. Kahn, D. Reidel, Dordrecht, 1985, pp. 389–420.
14 V. H. Crawford, H. W. Richardson, J. R. Wasson, D. J. Hodgson and W. E. Hatfield, *Inorg. Chem.*, 1976, **15**, 2107.
15 L. Merz and W. Haase, *J. Chem. Soc., Dalton Trans.*, 1980, 875.
16 J. Lorösch, U. Quotschalla and W. Haase, *Inorg. Chim. Acta*, 1987, **131**, 229.
17 S. M. Gorun and S. J. Lippard, *Inorg. Chem.*, 1991, **30**, 1625.
18 E. W. Ainscough, A. G. Bingham, A. M. Brodie, J. M. Husbands and J. E. Plowman, *J. Chem. Soc., Dalton Trans.*, 1981, 1701.
19 K. D. Karlin, A. Farooq, J. C. Hayes, B. I. Cohen, T. M. Rowe, E. Sinn and J. Zubieta, *Inorg. Chem.*, 1987, **26**, 1271.
20 M. Suzuki, H. Kanatomi, Y. Demura and I. Murase, *Bull. Chem. Soc. Jpn.*, 1984, **57**, 1003.
21 B. J. Hathaway, *Struct. Bonding (Berlin)*, 1984, **57**, 55.
22 G. M. Sheldrick, SHELXTL PLUS, Siemens Analytical X-Ray Instruments, Madison, WI, 1990.
23 G. M. Sheldrick, SHELXL 93, Program for Crystal Structure Determination, University of Göttingen, 1993.

Received 14*th March* 1995; *Paper* 5/01594D